



An Overview of Recent Advancement in the Three-Dimensional Limit Equilibrium Method and Its Implication on Slope Stability Analysis for Iron Ore Mining

Wensong Zhang^(✉) and Jan Janse van Rensburg

Rio Tinto Iron Ore, Perth, WA, Australia
wensong.zhang@riotinto.com

Abstract. With rapidly advancing computational technologies and more accessible high-performance computing machines in the past decade, the three-dimensional limit equilibrium (3D LE) method has become increasingly popular in the assessment of open pit slope stabilities. Unlike the Finite Difference (FD) and Finite Element (FE) methods, the accuracy of the LE method has significant reliance on its ability to accurately predict the shape (i.e., form) of the potential failure surface(s). Three recently proposed 3D slip surface searching algorithms and formulations were first discussed in this paper. Their effectiveness in facilitating more robust slope stability analyses were investigated with case examples that represent both rockmass and structurally controlled slopes from iron ore mines within the Pilbara region of Western Australia. By means of local surface optimisation, the surface-altering optimisation (SAO) algorithm was found to be highly effective in predicting slip surfaces of lower factor of safety (FoS). The multi-modal optimisation (MMO) algorithm was also proven useful in capturing multiple potential instability zones. Despite being able to provide more realistic predictions of the geometry and extent of the potential instabilities when performed in conjunction with SAO and MMO, the robustness of the new spline global surface search formulation could not be fully verified by the pit examples analysed in this study.

Keywords: 3D LEM · slope stability analysis · open pit · iron ore mining

1 Introduction

The Limit Equilibrium (LE) method has been used by engineering practitioners over the past century to perform slope stability analyses. By assuming and discretising potential failure surfaces (also known as ‘slip surfaces’) into multiple slices that satisfy force and/or moment equilibriums, the method searches for a slip surface that yields the lowest Factor of Safety (FoS). This searching process is realised via solving an optimisation problem by minimising the FoS using the geometric parameters that define the slip surfaces.

Compared to the more advanced Finite Element (FE) and Finite Difference (FD) methods, the LE method requires less configuration effort and is generally faster to

compute. However, the accuracy of this more simplified method relies heavily on its ability to find a sufficiently conservative yet realistic critical slip surface. Continuous efforts were made by generations of researchers and developers to improve the accuracy of the LE method, mostly by adopting more realistic assumptions on the calculation of inter-slice forces [1–4].

For many modern-day slope design applications, recent development of more robust surface-searching algorithms has made the 2D LE method more preferable than other numerical techniques by allowing engineering practitioners to analyse multiple design concepts and scenarios within matters of seconds and minutes.

While many slope stability problems can be approximated using the plane strain geometrical simplification adopted by the 2D LE method, the pursuit for more economic and profitable slope designs has made 3D LE analyses increasingly more desirable. Coupled with the emergence of increasingly affordable and robust high-performance computing devices over the past two decades, the 3D LE method has gradually gained popularity in the modelling of slope stability problems with complex 3D geometrical, geological or hydrogeological features.

1.1 Three-Dimensional Limit Equilibrium (3D LE) Method

Reliable geometrical approximation to failure surface(s) is crucial for the implementation of the 3D LE method, which requires a 3D surface formulation that contains sufficient degrees of freedom (DoF) to approximate possible instabilities. Traditionally, simplifications had to be made by adopting basic 3D geometry forms such as spheres and ellipsoids as a compromise for computational efficiency. This means, until recently, most 3D LE packages are only capable of capturing failure surfaces of spherical and ellipsoidal nature. This simplification is generally reasonable for predicting instabilities within isotropic and homogeneous materials, but may become less accurate when the potential slip surface travels through multiple material layers or materials of complex anisotropies.

In the context of typical iron ore mining, the sphere and ellipsoid surface formulations tend to produce more reliable results when used for modelling of waste dumps and landbridges, as well as instabilities that are governed by rockmass failures in relatively homogenous and isotropic materials. However, they are often considered being less accurate in approximating structurally controlled planar sliding failure surfaces that are commonly seen in the banded iron formations (BIF), nor being able to predict the full extent of the zone of potential instability.

Moreover, many slope instabilities are governed by local variations of bedding structures in iron ore mining. It is thus important for designers to be able to identify all pit sectors with FoS values that may fail to meet relevant design acceptance criteria (DAC). Unfortunately, traditional 3D LE search methods (e.g., Cuckoo [5]) can often only locate a single zone of potential instability from each analysis, and requires specific search limits to be prescribed for the assessment of different slope sectors.

This paper aims to provide an overview of three recently developed slip surface searching algorithms and formulations proposed to address the abovementioned challenges in 3D LE modelling. This is followed by two case examples of typical slopes

from iron ore mines in the Pilbara region of Western Australia, to provide insights on the effectiveness of these recent advancements.

2 Recent Advancements in 3D Slip Surface Searching

The following algorithms and formulations were published in recent years to help locate zones of potential instabilities more accurately and efficiently in 3D LE analyses.

2.1 Multi-Modal Optimisation (MMO)

Traditional LE slope stability analysis methods seek to locate single critical slip surface (i.e., the global minimum for FoS). While this is generally sufficient for most 2D LE applications where the analyses are performed at critical slope locations identified by the designers, the capability to identify multiple local minima is highly desirable in 3D LE analyses to help locate all zones of potential instabilities, which in turn can facilitate more effective management of design risks.

The concept of multi-modal optimisation (MMO) was proposed based on the locally informed particle swarm (LIPS) optimisation technique developed by Qu et al. (2012) [8] for the particle swarm optimisation (PSO) algorithm [6]. Recently, Li et al. (2020) [9] introduced a radius filter to allow the method to specify the minimum distance between any local minima (i.e., the LIPS-R method), which forms the basis of the MMO functionality in Rocscience Slide3. During the global surface search process, the algorithm may be utilised to help locate multiple local minima across the model space, as shown by the example schematic in **Fig. 1**.

It is worthwhile noting that the MMO feature may only be used in conjunction with the Particle Swarm Search (PSS) method, which is traditionally less commonly used than the Cuckoo search method in performing single-minimum analyses.

2.2 Surface-Altering Optimisation (SAO)

To date, 3D global surface search algorithms can still only operate with a relatively small number of degrees of freedom (DoF) as a compromise for higher computational efficiency. This means the global search results that assume spherical and ellipsoidal slip surfaces often overestimate the FoS due to the lack of DoF to approximate the actual critical slip surface(s).

Local surface optimisation by means of the surface-altering optimisation (SAO) method was first developed for 2D LE [10] before being extended into 3D by Ma et al. (2022) [11]. The algorithm performs local surface optimisation on the global search results (see **Fig. 1**) to improve accuracy. Before the SAO can commence, the spherical or ellipsoidal surface identified by the global search is first converted in a nonuniform rational basis spline (NURBS), which is a geometrical approximation process that turns a surface into quadratic splines of the second polynomial degree. This process significantly increases the DoF in geometrical approximation of slip surfaces. A total of five geometric manipulation steps are then performed on the derived NURBS in an iterative manner, to allow for local optimisation of the global search result.

It may be noted that approximation error from surface-to-NURBS conversion may cause the FoS to slightly increase [11]. In earlier versions of Rocscience Slide3, this had led to higher FoS being reported by analyses with SAO enabled, especially in cases where the expected critical slip surface is spherical or ellipsoidal (i.e., in generally homogenous and isotropic materials). A recent software update has fixed this issue by reporting the global surface search result instead, if the SAO returned no improvement in FoS.

2.3 Spline Formulation for Global Surface Search

While the invention of SAO has allowed for localised searching of more complex slip surface geometries, its effectiveness relies heavily on the zone(s) of potential instability being accurately located by the global surface search. As illustrated in Fig. 1, the overly simplified spherical and ellipsoidal surface formulations may prevent the global search algorithm from locating one or more critical slope areas, and therefore significantly reduce the chance of locating the global minimum.

The incorporation of a spline formation in the global surface search process was proposed by Ma et al. (2022) [12], where a total of eleven parameters are used to define a slip surface. This is to be compared to 4 parameters used to define a spherical surface. The increase in DoF in slip surface formation, in theory, should facilitate more accurate identification of critical slope area(s) during the global search stage, and therefore lead to improvement in overall accuracy of the analyses.

In addition, the surface(s) found using the spline formulation during the global search stage can be readily used for SAO without further NURBS conversion, hence eliminating the potential increase in FoS caused by the approximation error.

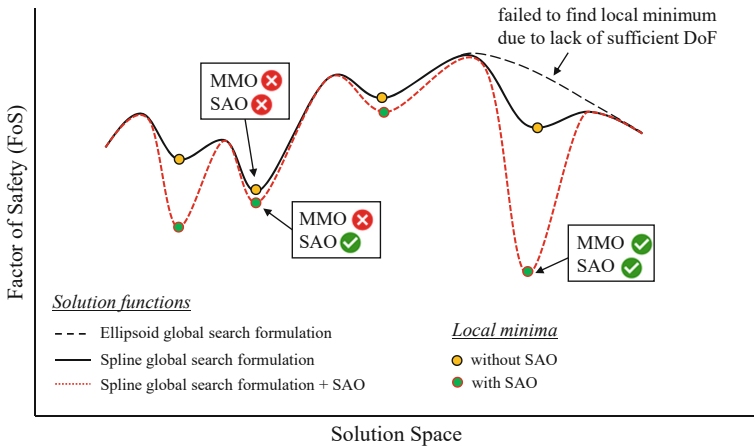


Fig. 1. Example schematic of the effect of the algorithms and formulations discussed in this paper

3 Case Examples

The following iron ore mining slope examples were used to study the effectiveness of MMO, SAO and spline surface formulations recently introduced to Rocscience Slide3 (version 3.020) [7].

The analyses were performed using both GLE/Morgenstern-Price and Janbu Simplified methods, while only results from the GLE/Morgenstern-Price method were reported in this paper. No search limit was defined. As per default setting in Rocscience Slide3 (version 3.020) [7], the MMO analyses were configured to use 20 particles to report up to 3 local minima that are at least 10% of model space distance away from one another. Default convergence parameters were also adopted for the SAO analyses.

3.1 Pit Example 1

Pit Example 1 represents a typical rockmass controlled open-pit slope. As shown in **Fig. 2**, the slope is predominantly exposed in detrital units, which are underlaid with flat-bedded bedrock units. The properties of the main geological units can be described as following:

- Unit A and B are relatively competent material of borderline rock strength;
- Unit C and D are clay rich units of low to high plasticity;
- Unit E and F are soil strength units of varying clay/shale content; and
- Unit G and below are weathered bedrock units and are significantly stronger than Unit A-F.

The pit slope incorporates wider berms on 640RL and 670RL, as well as two minor bull-nose features below the 670RL berm. The FoS and slip surface(s) predicted from a series of 3D LE analyses completed on this pit example are summarised **Table 1** and **Fig. 3**, respectively.

The Effect of MMO. In absence of MMO, a single minimum of 1.08 was identified by the traditional Cuckoo search method. The critical slip location is close to one of bull-nose features, implying borderline double-batter stability within the weaker Unit C material. When the Particle Swarm Search (PSS) method was used, the analysis yielded a critical slip surface within upper slope, reporting a higher FoS of 1.21. The divergence in critical slip surface prediction by the two global search methods indicates, for a model of such complexity, multiple local minima are likely to exist.

When MMO was performed using the PSS search method, the analysis identified a second local minimum adjacent to the critical slip surface (FoS = 1.33), as well as a third one (FoS = 1.43) within the same bullnose feature as predicted by the Cuckoo search method. However, the results are both significantly less conservative (i.e., predicting higher FoS values) than the single minimum reported by the traditional Cuckoo search method.

The Effect of SAO. Both Cuckoo and PSS search methods reported similar critical surface locations to those predicted without SAO. However, the lowest FoS are now reported as 0.66 and 1.09, respectively, implying a potential double-batter instability at the bullnose. It is evident from the significant FoS reduction that the incorporation

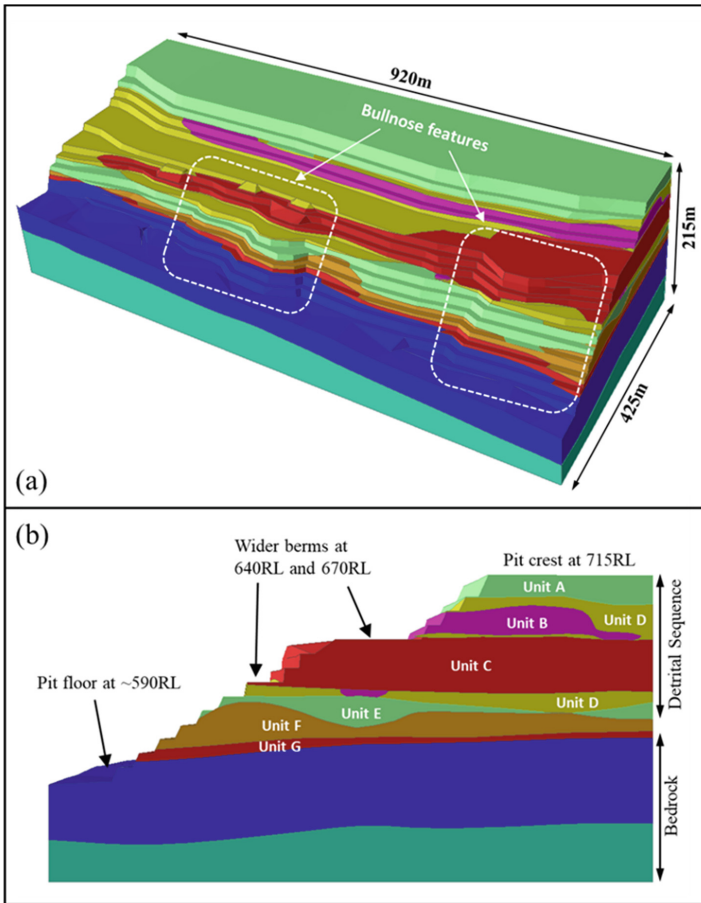


Fig. 2. Overview of Pit Example 1 and the assumed geology model

of local surface optimisation by means of SAO had led to significantly more conservative estimations on the stability of the analysed slope. The additional geometrical DoF from the NURBS approximation of slip surfaces as well as the proposed optimisation procedures are thus found to be highly effective.

It is worthwhile noting that when both SAO and MMO were performed using the PSS method, the analysis reported a new critical slip surface near the bullnose, at a much lower FoS of 0.75. Instead of performing local optimisation on a single minimum, the MMO provided opportunity for SAO to be performed at all local minima identified from the global surface search stage, and allowed for the capturing of more conservative slip surfaces with lower FoS values.

The Effect of Spline Global Search. Surprisingly, the critical FoS calculated with both Cuckoo and PSS search methods increased despite the additional geometrical DoF incorporated by the spline surface formulation. Neither search method predicted any potential double-batter instability (i.e., $\text{FoS} < 1$) at the bullnose.

Table 1. Summary of FoS values predicted by the 3D LE analyses for Pit Example 1

	Cuckoo Search		Particle Swarm Search			
	Single Minimum		Single Minimum		Multi-Modal Optimisation	
	Ellipsoid	Spline	Ellipsoid	Spline	Ellipsoid	Spline
No Surface-Altering Optimisation	1.08	1.29	1.21	1.19	1.21	1.19
					1.33	1.29
					1.43*	1.32
With Surface-Altering Optimisation	0.66*	1.22	1.09	1.17	0.75*	1.13
					1.10	1.17
					1.13	1.17

*slip surface near bullnose below the 670RL decoupling berm

Compared to the ellipsoid surface formulation, smaller SAO-induced reductions in FoS could be observed with the spline surface formulation. This is expected as the extra DoF from the spline surface formation should bring the global search outcome closer to results that were locally optimised (by SAO).

When MMO was performed, the search with spline surface formulation seemed to have focused on the upper slope above the 670RL berm, with no indication of any potential double-batter instability within the lower slope bullnose area. It appears the increased geometrical DoF incorporated by the spline global surface formulation may have led to an increased number of slip surfaces of similar FoS being identified within the upper slope, which dominated the search focus. A subsequent study conducted by Rocscience [14] indicated that, by increasing both number and minimum radius span of the local minima adopted by MMO, searches performed using the spline surface formulation were able to capture the potentially more critical double-batter instability.

As expected, the more complex spline surface formulation has allowed for slip surfaces of much larger aspect ratios to be formed. Together, the 3 slip surfaces identified from the MMO analysis have covered the entire upper slope. This provides a more realistic representation of the extent of the potential instability, given the lack of 3D geometrical and geological features in the upper slope.

For this pit example, the results predicted with spline surface formulation are generally found to be less conservative (i.e., of higher FoS values) than those predicted using the traditional ellipsoid surface formulation.

3.2 Pit Example 2

The second pit example represents typical structurally controlled slopes within the Banded Iron Formation (BIF), where planar sliding along major shale bands is the dominating failure mechanism. As shown in **Fig. 4**, the bedding surfaces dip into the pit at 20°–50°. The geology setting can be summarised as following:

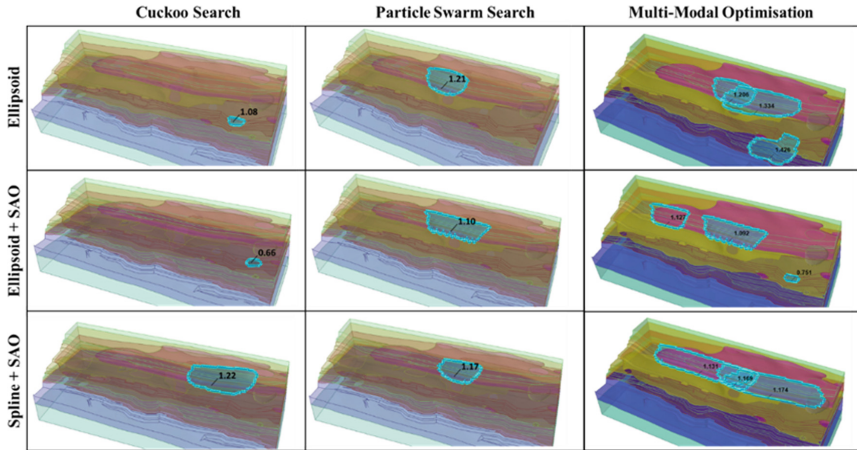


Fig. 3. Critical slip surfaces and their corresponding FoS values predicted by the 3D LE analyses for Pit Example 1

- Unit X and Unit Y are both sedimentary rock units with interbedded shale and BIF layers;
- Unit X becomes mineralised towards the bottom of the slope, where the material is expected to be heavier yet weaker in strength; and
- The slope is intersected by a fault system, which introduced a minor offset in the geology sequence.

In general, the slope design adopted a batter-berm configuration except for the dip slope mining section below 640RL, where a higher risk of instability is expected due to relatively low material strength, unfavourable bedding angles and potential daylighting of major shale bands. Lower bound rockmass and defect shear strength parameters were adopted in the analyses, together with ubiquitous modelling of shale band anisotropy to account for structural uncertainty.

The FoS and slip surface(s) predicted from a series of 3D LE analyses completed on this pit example are summarised **Table 2** and **Fig. 5**, respectively.

The Effect of MMO. When ellipsoidal surfaces were searched with no subsequent local optimisation, the cuckoo and PSS global search methods yielded FoS of 1.38 and 1.24, respectively. The critical search surfaces were both located within (or partially within) the dip slope mining section and are of circular nature when projected onto the pit surface.

When MMO was performed in the analysis, two further local minima were located that are in proximity to previous critical slip surface found by the PSS method, with significantly higher FoS of 1.61 and 1.62.

The Effect of SAO. For single minimum searches, the cuckoo and PSS global search methods now report FoS of 1.05 and 1.02, respectively, showing significant reductions from previous analyses where no local surface optimisation was performed. The geometry of the predicted slip surfaces is also of higher aspect ratios, better resembling a potential planar sliding instability.

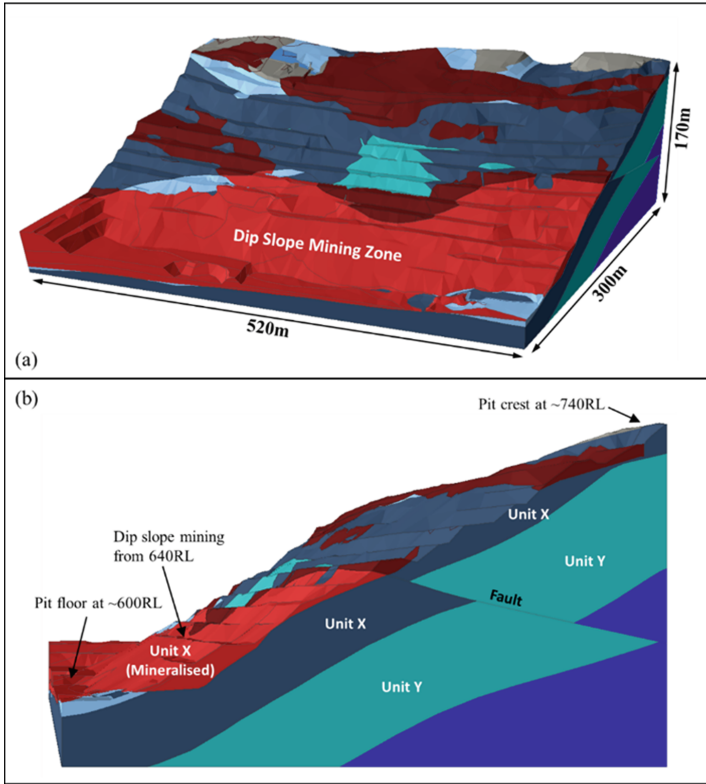


Fig. 4. Overview of Pit Example 2 and the assumed geology mode

Table 2. Summary of FoS values predicted by the 3D LE analyses for Pit Example

	Cuckoo Search		Particle Swarm Search			
	Single Minimum		Single Minimum		Multi-Modal Optimisation	
	Ellipsoid	Spline	Ellipsoid	Spline	Ellipsoid	Spline
No Surface-Altering Optimisation	1.38	1.35	1.24	1.53*	1.24	1.49
					1.61	1.98
					1.62*	1.99*
With Surface-Altering Optimisation	1.05	1.14	1.03	1.48*	1.02	1.03
					1.24	1.48*
					1.34*	

*slip surfaces outside of the dip slope mining section

In the case where MMO was also performed, an additional local minimum was identified within the batter-berm slope section, reporting a FoS of 1.34. The results again suggest that the critical slip surface(s) identified by the global surface search process may be unconservative and can considerably overestimate the FoS.

The Effect of Spline Global Search. Using the Cuckoo search method, the FoS predicted with the ellipsoid and spline surface formulations are generally comparable, with and without SAO. Surprisingly, when the PSS global search method was used (in absence of MMO), the spline surface formulation did not locate a critical slip surface within the dip slope mining section, and reported FoS values of up to 40% higher than those from the less complex ellipsoid surface formulation. A similar observation can be made when MMO was performed without SAO, where an average 20% increase in FoS was observed for all three local minima. More comparable results were reported by Rocscience [14] in a subsequent study, after improving the search coverage by increasing the number of PSS particles from 20 (i.e., software default) to 25.

When MMO and SAO were both performed in addition to the spline surface formulation, the analysis was able to predict a critical planar sliding slip surface within the dip slope mining section, at a comparable FoS (1.03) to that from the ellipsoid surface formulation (1.02). Moreover, the critical slip surface predicted using the spline global surface formulation has a significantly larger footprint, indicating the entire dip slope mining section is at a FoS of 1.03.

Benchmarking against the Finite Element (FE) method. A further 3D FE analysis was conducted for Pit Example 2 using Rocscience RS3 (version 4.026) to provide benchmark to the 3D LE analyses. As shown in Fig. 6, the 3D FE model was configured to have the same extent as the 3D LE model, with roller fixity assigned to all side faces while fully fixing the bottom.

The model was meshed with a total of 311346 s order (i.e., 10-noded) tetrahedral elements. A refined mesh was adopted near pit surface to provide higher accuracy in the modelling of surficial planar sliding that was predicted by the 3D LE method. A

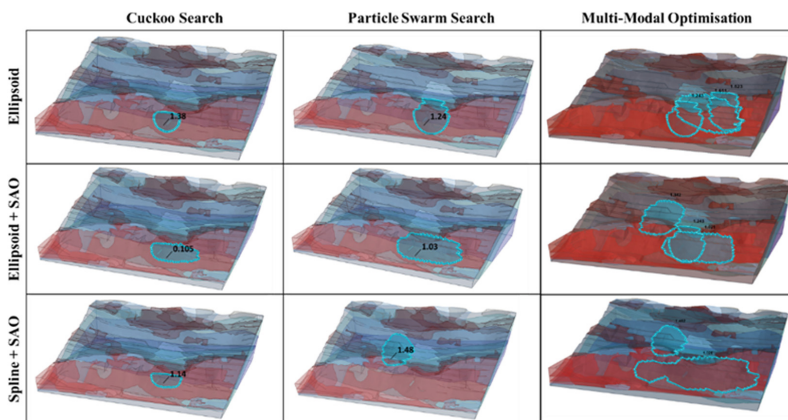


Fig. 5. Critical slip surfaces and their corresponding FoS values predicted by the 3D LE analyses for Pit Example 2

Table 3. Convergence parameters adopted in the 3D FE analysis for Pit Example 2

Simulation Stage	Convergence Type	Max. No. Iterations	Tolerance
Stress Analysis	Absolute Force and Energy	300	0.001
Shear Strength Reduction			

sensitivity study was first completed on mesh size and convergence parameters to ensure sufficient numerical accuracy has been achieved.

To calculate the critical strength reduction factor (SRF), shear strength reduction (SSR) was performed on both rockmass and defect strength parameters. The adopted convergence conditions and parameters are summarised in **Table 3**.

The critical SRF was found to be 1.05, predicting a planar sliding within the dip slope mining section. This is to be compared to a critical FoS of 1.03 from the 3D LE analysis (incorporating MMO, SAO and spline surface formulation). The total displacement and maximum shear strain contour plots are shown in **Fig. 6** for $SRF = 1.05$, which are overlaid with the slip surfaces predicted by 3D LE analyses. Large shear strains were predicted near the toe of the slope within the dip slope mining section, with a comparable lateral extent to that of the critical slip surface predicted by the 3D LE analysis (incorporating MMO, SAO and spline search formulation).

A further comparison can be made by examining six 2D cross-sections within the dip slope mining section, as shown in **Fig. 7**. A planar sliding shear surface can be clearly seen to follow the bedding surface. The depth, extent and spatial variation of this shear surface are found to be in strong agreement with the critical slip surface predicted by the 3D LE analysis that incorporated MMO, SAO and the spline surface formulation.

The simulation time taken to perform the 3D LE and 3D FE analyses are summarised in **Table 4**. All simulations were completed on a laptop with an Intel Xeon W-11855M CPU and 128GB RAM. Although an increase in computational effort was required to facilitate MMO in the 3D LE analysis, the total computation time remain less than a tenth of that for a single 3D FE analysis ($SRF = 1.05$).

4 Conclusions

An overview was provided on three recent advancements made to the 3D LE method (i.e., MMO, SAO and the spline surface formulation), followed by two case examples from a typical iron ore mining environment to investigate the effectiveness of the involved 3D slip surface searching algorithms and formulations.

In both the rockmass and structurally controlled pit examples, the local surface optimisation algorithm performed using SAO was able to significantly reduce the FoS predicted from the global surface search. While the MMO algorithm can only be performed with the PSS method, it successfully captured multiple zones of potential instability in both pit examples, and is considered a useful tool for the assessment of larger slope models of variable geometrical, geological and hydrogeological conditions. Using the default search parameters adopted by Rocscience Slide3 (version 3.020) [7], this study

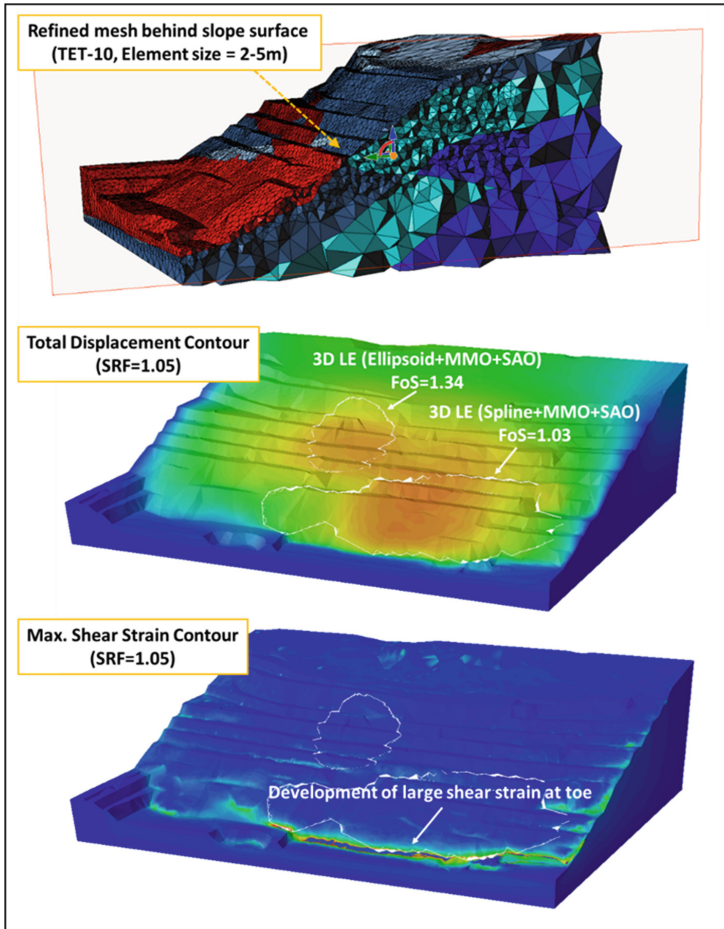


Fig. 6. Mesh adopted by the 3D FE analysis for Pit Example 2 and contour plots of predicted displacement and maximum shear strain at SRF = 1.05

Table 4. Comparison of simulation time required to complete the 3D LE and 3D FE analyses for Pit Example 2

Method	Software	Simulation Type	Simulation Time (seconds)
3D LEM	Rocscience Slide3	PSS(MMO), SAO, Spline	1,463
		Cuckoo, SAO, Spline	427
3D FEM	Rocscience RS3	SSR	18,746*

*Simulation time for the SRF = 1.05 step

was unable to verify the effectiveness of the spline surface search formulation in predicting more conservative slip surfaces (i.e., with lower FoS values). While in theory the

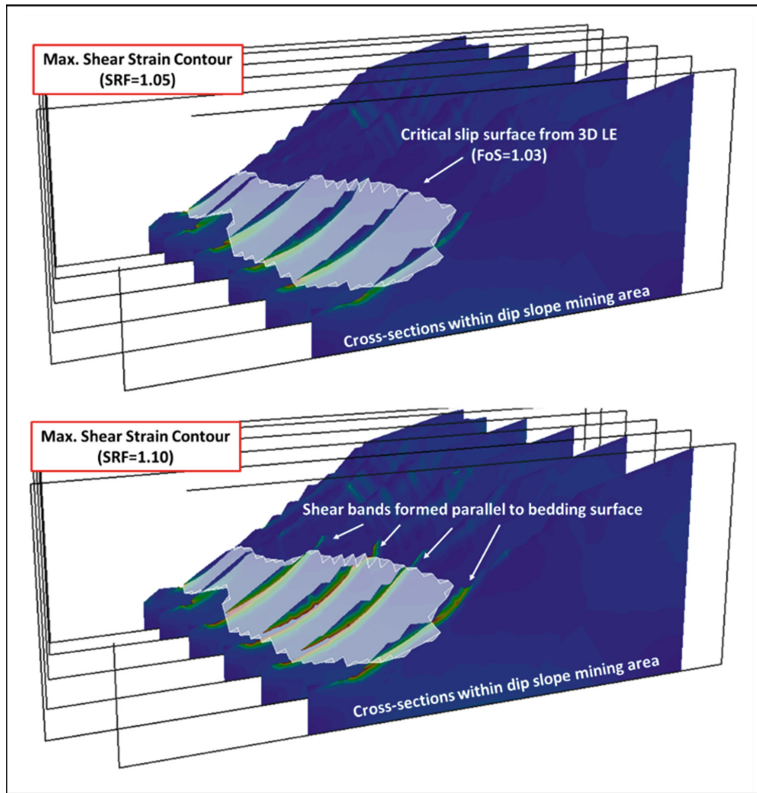


Fig. 7. Comparison of failure surfaces predicted by the 3D FE and 3D LE methods for Pit Example 2

additional geometrical DoF should improve the robustness of global surface search, the reported critical FoS are generally found to be similar or in some cases higher than those predicted using the traditional ellipsoid surface formulation, especially in absences of MMO and SAO. However, the new formulation does provide significant improvement in predicting the geometry and extent of the potential zones of instability, as confirmed by the FE analysis performed on Pit Example 2.

Lastly, it is important to recognise that a critical slip surface identified by the LE method must not be seen as an upper- or lower- bound solution. Fundamentally, this is because there is no stress or displacement field calculations incorporated, and hence the static and kinematic admissibility requirements from the classic limit theorems cannot be satisfied or verified [13]. This has two important implications:

- Not all slip surfaces predicted by the LE method are realistic; and
- A slip surface of lower FoS is not necessarily more 'correct', but only more 'conservative' from a risk management perspective.

While the rapidly evolving LE algorithms and formulations always promise to find slip surfaces of lower FoS, the responsibility remains with the users to determine how probable it is for them to occur in the real world.

Acknowledgement. The authors would like to thank Alison McQuillan and the Rocscience Technical Support team for their help in troubleshooting the 3D LE and FE models referenced in this paper.

References

1. Bishop, A.W. "The use of the slip circle in the stability analysis of slopes." *Geotechnique* 5.1 (1955): 7–17.
2. Janbu, N. "Slope stability computations." Publication of: Wiley (John) and Sons, Incorporated (1973).
3. Spencer, E. "A method of analysis of the stability of embankments assuming parallel inter-slice forces." *Geotechnique* 17.1 (1967): 11–26.
4. Fredlund, D.G. "The relationship between limit equilibrium slope stability methods." 10th. ICSMFE, 1981 3 (1981): 409–416.
5. Yang, X.S., Deb, S. "Cuckoo search via Lévy flights." 2009 World congress on nature & biologically inspired computing (NaBIC). Ieee, 2009.
6. Kennedy, J., and Russell, E. "Particle swarm optimization." *Proceedings of ICNN'95-international conference on neural networks*. Vol. 4. IEEE, 1995.
7. Rocscience, Slide3 Maintenance+ Update History (Version 3.020), <https://www.rocscience.com/support/slide3/release-notes>, last accessed 19/02/2023.
8. Qu, B.Y., Suganthan, P.N. and Das, S. "A distance-based locally informed particle swarm model for multimodal optimization." *IEEE Transactions on Evolutionary Computation* 17.3 (2012): 387–402.
9. Li, S., Cami, B., Javankhoshdel, S., Corkum, B., Yacoub, T. "Considering multiple failure modes in limit equilibrium slope stability analysis: Two methods." *GeoVirtual 2020*, the Canadian Geotechnical Society (2020).
10. Mafi, R., Javankhoshdel, S., Cami, B., Chenari, R. J., and Gandomi, A.H. "Surface altering optimisation in slope stability analysis with non-circular failure for random limit equilibrium method." *Georisk: Assessment and Management of Risk for Engineered Systems and Geohazards* 15, no. 4 (2021): 260–286.
11. Ma, T., Mafi, R., Cami, B., Javankhoshdel, S. and Gandomi, A.H. "NURBS Surface-Altering Optimization for Identifying Critical Slip Surfaces in 3D Slopes." *International Journal of Geomechanics* 22, no. 9 (2022): 04022154.
12. Ma, T., Cami, B., Javankhoshdel, J., Corkum, B., and Yacoub, T. Optimization of spline slip surfaces using metaheuristic search in LEM. In *Proceedings of the TMIC2022 Slope Stability Conference*, Atlantic Press (Springer Nature) (2022).
13. Drucker, D.C., William Prager, and Harvey J. Greenberg. "Extended limit design theorems for continuous media." *Quarterly of applied mathematics* 9.4 (1952): 381–389.
14. Rocscience, peer review report (2) for RIC2023 paper submission titled 'An overview of recent advancement in the three-dimensional limit equilibrium method and its implication on slope stability analysis for iron ore mining' (2023).

Open Access This chapter is licensed under the terms of the Creative Commons Attribution-NonCommercial 4.0 International License (<http://creativecommons.org/licenses/by-nc/4.0/>), which permits any noncommercial use, sharing, adaptation, distribution and reproduction in any medium or format, as long as you give appropriate credit to the original author(s) and the source, provide a link to the Creative Commons license and indicate if changes were made.

The images or other third party material in this chapter are included in the chapter's Creative Commons license, unless indicated otherwise in a credit line to the material. If material is not included in the chapter's Creative Commons license and your intended use is not permitted by statutory regulation or exceeds the permitted use, you will need to obtain permission directly from the copyright holder.

